Effect of land-sea air masses transport on spatiotemporal distributions of atmospheric CO_2 and CH_4 mixing ratios over the south Yellow Sea

Jiaxin Li [1], Kunpeng Zang [1,2,3]*, Yi Lin [1], Yuanyuan Chen [1], Shuo Liu [1], Shanshan Qiu [1], Kai Jiang [1], Xuemei Qing [1], Haoyu Xiong [1], Haixiang Hong [1], Shuangxi Fang [2,4]*, Honghui Xu[5], Yujun Jiang[5]

[1] *College of Environmental and Resources Sciences, Zhejiang University of Technology, Hangzhou, China*, [2] *Zhejiang Carbon Neutral Innovation Institute, Zhejiang University of Technology, Hangzhou, China*, [3] *National Marine Environmental Monitoring Center, Dalian, China*, [4]*Collaborative Innovation Center on Forecast and Evaluation of Meteorological Disasters (CIC-FEMD), Nanjing University of Information Science & Technology, Nanjing, China*, [5] *Zhejiang Meteorological Science Institute, Hangzhou, China*

Corresponding to: Kunpeng Zang (zangkunpeng@zjut.edu.cn), Shuangxi Fang (fangsx@zjut.edu.cn)

Abstract: To reveal the spatiotemporal distributions of atmospheric CO_2 and CH_4 mixing ratios and regulation mechanisms over the China shelf sea, two field surveys were conducted in the south Yellow Sea in China in November 2012 and June 2013, respectively. Observed results showed that mean background atmospheric CO_2 and CH_4 mixing ratios were 403.94 (13.77) ppm and 1924.8 (27.8) ppb in November 2012, and 395.90 (3.53) ppm and 1918.0 (25.7) ppb in June 2013, respectively. An improved data filtering method was optimized and established to flag atmospheric CO_2 and CH_4 emission from different sources in survey area. We found that, the spatiotemporal distributions of atmospheric CO_2 and CH_4 mixing ratios over the south Yellow Sea were dominated by land-sea air masses transport, which was mainly driven by seasonal monsoon, while the influence of air-sea exchange was negligible. In addition, atmospheric CO_2 and CH_4 mixing ratios over the south Yellow Sea could be elevated remarkably in a distance of approximate 20 km offshore by land-to-sea air masses transportation from the Asia Continent

during early winter monsoon.

Keywords: carbon dioxide, methane, monsoon, marine boundary air, shipborne underway measurement.

1 Introduction

Carbon dioxide (CO_2) and methane (CH_4) are the two most important greenhouse gases, playing critical roles in Earth's radiation balance (AGGI, 2014; WMO greenhouse gas bulletin, 2022). Since the industrial revolution era (~1750), atmospheric CO_2 and CH_4 mixing ratios have been increasing, and reached their highest values of 415.7 ± 0.1 ppm and 1908 ± 2 ppb in 2021, which were about 149% and 262% of the preindustrial levels (WMO greenhouse gas bulletin, 2022). Increasing of atmospheric CO_2 and CH_4 was unequivocally attributed to anthropogenic emissions, e.g., industrial production, deforestation, fossil fuel consumption (Houghton, 2003; Peters et al., 2012), and natural source-sink processes (Zang et al., 2017).

For decades, spatiotemporal distributions of atmospheric CO_2 and CH_4 mixing ratios have attracted more and more attention from science community. Shipborne observation was considered as one of six common and important methods for observing greenhouse gases (Matsueda et al., 1996; Daube et al., 2002; Dlugokencky et al., 2005; Crosson, 2008; Fang et al., 2015). Based on shipborne discrete sampling and measurement, latitudinal distribution of CH_4 mixing ratio with a sharp drop in the area of 20 °N in marine boundary air of the North Pacific Ocean were reported, which was mainly influenced by air masses transportation driven by both winter monsoon and trade wind (Matsueda et al., 1996; Dlugokencky et al., 2005). In coastal area of the Bohai Sea, seasonal variations of atmospheric CO_2, CH_4 and N_2O mixing ratios were mainly influenced by land-sea air masses transportation based on discrete sampling observation (Kong et al., 2010). Moreover, periodic observed CO_2 and CH_4 mixing ratios in marine boundary air were also used to improve the accuracy of calculated air-sea CO_2 flux in the northern South China Sea and the Luzon Strait (Zhai et al., 2015), and assess impacts of several episodic oil and gas spill events on abnormal air-sea CH_4 flux in the Bohai Sea (Zhang et al., 2014).

In recent years, high-accuracy and high-resolution shipborne continuous observation method has been developed and applied to observe greenhouse gases in marine boundary air (Nara et al., 2014; Zang et al., 2017; Reddick et al., 2019), which could reveal more detailed information associated with their source-sink processes. Latitudinal distributions of both CO_2 and CH_4 mixing ratios in the China shelf sea boundary air in early spring were observed, which were similar to that in the north Pacific Ocean (Matsueda et al., 1996; Zang et al., 2017), and mainly impacted by atmospheric chemical processes, air-sea interaction in Yangtze River estuary area and land-sea air masses transportation (Zang et al., 2017; Liu et al., 2018). Meanwhile, peak values of CO_2 and CH_4 mixing ratios in downwind area of offshore oil and gas platforms, which were recognized as hot spot sources of greenhouse gases, were observed by shipborne continuously measurement systems in the North Sea, the South China Sea and Bohai Sea. Combined with the Gaussian plume model, CH_4 emissions could be quantified via “top-down” approach (Nara et al., 2014; Riddick et al., 2019; Zang et al., 2020).

Monsoon is a kind of climatic phenomenon in which the dominant wind system changes with seasons (Lyu et al., 2021). The East Asian monsoon (EAM), comprising the East Asian summer monsoon (EASM) and East Asian winter monsoon (EAWM), is an important component of the Earth’s climate system and significantly influences the socioeconomic, agricultural and cultural development of East Asia (Huang, 1985; Zou et al., 2018; Lyu, et al., 2021). Previous studies have shown that the East Asian monsoon played an important role in global and regional climate variability (Huang, 1985; Chang et al., 2000; Ding et al., 2007; Zhan and Li, 2008). On the one hand, spatiotemporal distributions of CO_2 and CH_4 in marine boundary air were influenced by multiple processes, such as land-sea air masses transport (Bartlett et al., 2003; Zang et al., 2017), ship emission (Warnekeet et al., 2005; Law et al., 2013; Bouman et al., 2017; Ding et al., 2018) and oil and gas platforms (Nara et al., 2014; Reddick et al., 2019; Zang et al., 2020). On the other hand, greenhouse gases have been observed and studied in East Asia and Pacific Ocean based on land (island)-based stations (Fang et al., 2015; 2017; Luan et al., 2016), ship and plane observation platforms for many years (Matsueda et al., 1996; Bartlett et al., 2003; Dlugokencky et al., 2005). However, as an important pathway of atmospheric components transportation between the Asia Continent and Pacific Ocean, spatiotemporal distributions and regulation mechanisms of CO_2 and CH_4 in the China shelf seas boundary air were still rare (Zhang et al., 2007; Zang et al., 2017; Liu et al., 2018).

In this study, atmospheric CO_2 and CH_4 mixing ratios in boundary air of the South Yellow Sea (SYS) were simultaneously observed by a self-assembled shipborne CRDS (Cavity Ring-down Spectroscopy, Picarro G2301, USA) system in November 2012 and June 2013, when typical periods of the EASM and the EAWM. The major objectives of this work were (1) to optimize an improved data filter approach for shipborne continuous mobile observation of atmospheric CO_2 and CH_4 mixing ratios, (2) to investigate the influence of air-sea exchange on the spatiotemporal distributions of CO_2 and CH_4 mixing ratios, and (3) to reveal the regulating mechanisms of seasonal monsoon on spatiotemporal distributions of CO_2 and CH_4 in marine boundary air of the SYS during the field surveys.

2 Method and materials

2.1 Observation area

The Yellow Sea is a semi-enclosed marginal sea, located on the western part of the Pacific Ocean, adjacent by China to the north and west, and Korean Peninsula to the east (Zhang and Chu, 2018; Wang et al., 2021). It is a main pathway of air mass transport between the Asia continent and Pacific Ocean, and can be divided into two basins: the North Yellow Sea (NYS) and the SYS (Lyu et al., 2021). The SYS covers an area of about 10.8×10^4 km^2, with an average depth of 44 m, and is strongly influenced by the EAM system (Zou et al., 2018). As showed in Fig. 1, to study the distributions of atmospheric CO_2 and CH_4 mixing ratios and their regulation mechanisms, two campaigns were conducted from 2^{nd} to 8^{th} November, 2012 and from 22^{nd} to 29^{th} June, 2013, respectively, when the typical periods of the EAM (including summer monsoon and winter monsoon). In order to ensure the comparability of observations, parallel observed CO_2 and CH_4 data from the three land (island)-based stations (LAN, JGS, TAP) located in vicinity area, were presented and studied in this study.

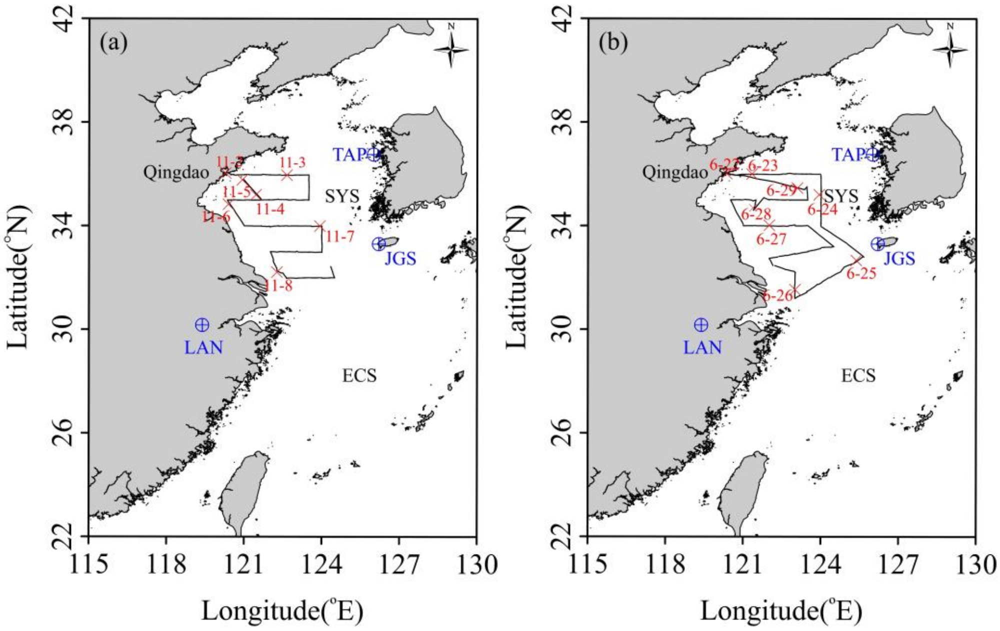

Fig. 1. Observation area in the SYS. The thick solid black lines represent cruise tracks in November 2012 (a) and June 2013 (b). Symbols represent the Tae-ahn Peninsula station (TAP, 36.73 °N 126.13 °E, 20 m above sea surface)，Jeju Gosan station (JGS, 33.30 °N 126.20 °E, 25 m above sea surface) and Lin'an station (LAN, 30.18 °N 119.44 °E, 138 m above sea surface), respectively (https://www.esrl.noaa.gov/gmd/dv/site/site_table.html). ECS represents the East China Sea. The Red Crosses represent the beginning locations of each natural day.

2.2 Measurement of atmospheric CO_2 and CH_4 mixing ratios

As showed in Fig. 2a, during the field surveys, the air inlet was fixed at the highest point of the bow, about 10 meters above the sea surface, and near the meteorological sensors for avoiding anthropogenic contamination (Zang et al., 2017). Atmospheric CO_2 and CH_4 mixing ratios were measured by using a self-assembled Picarro system (G2301, Picarro Inc., USA). The Picarro analyzer, which can acquire one measurement every 5 seconds, and correct the measurements influenced by water vapor (Rella et al., 2013), has been proven to be excellent for measuring CO_2 and CH_4 with high precise and accuracy (Crosson, 2008; Fang et al., 2013).

As showed in Fig. 2b, ambient air was pumped via the dedicated tube by an external vacuum pump, and passed through a membrane filter (1.0 μm, Whatman Inc., USA), a drying-tube filled with magnesium perchlorate [$Mg(ClO_4)_2$] and another filter, respectively, to remove particles and water vapor. Then, regulated by valve sequence setting, dry and clean air sample as well as the standard gases flowed into the CRDS analyzer through 8 port multi-position valve (Valco

Instruments Co. Inc. USA) with a flow rate of 200 mL·min^{-1} controlled by a mass flow controller (Beijing Seven-star electronics Co. LTD. China). Before and after each campaign, the CRDS analyzer was calibrated to guarantee its normal operation status. During field surveys, three standard gases were automatically measured in sequence each day, which was regulated by the CRDS analyzer. Linear functions were yielded based on measurement results and standard values of three standard gases, i.e., 254.53 (0.06) ppm, 365.14 (0.06) ppm and 569.99 (0.08) ppm for CO_2, and 1601.0 (0.8) ppb, 1925.5 (0.8) ppb and 2317.7 (0.5) ppb for CH_4, respectively, which were used to calibrated the observed data. The used standard gases were propagated from the WMO primary standards (WMO/GAW 2004 scale for CH_4, 2007 scale for CO_2), to guarantee the consistency, trace ability and international comparability of observed data (Dlugokencky et al., 2005).

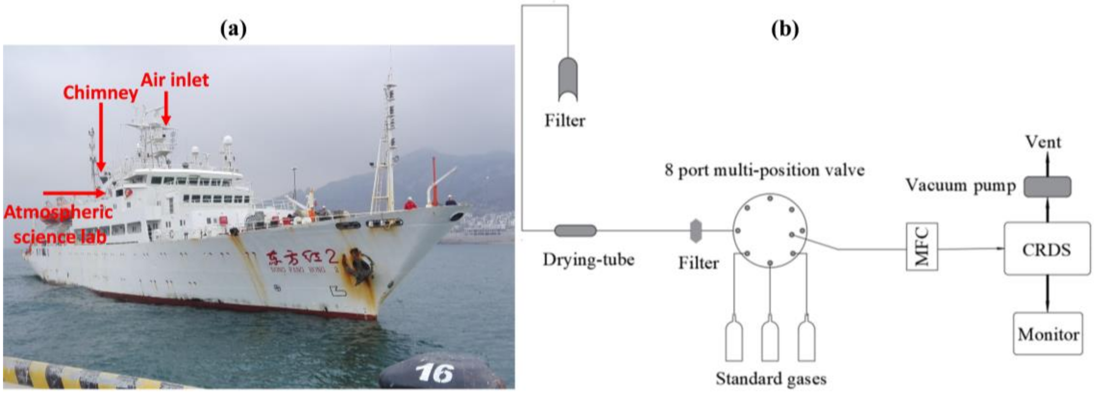

Fig. 2. The RV Dongfanghong Ⅱ (a). Schematic diagram of the shipborne Picarro system for observing atmospheric CO_2 and CH_4 (b).

2.3 Meteorological data

Both of the two campaigns were conducted by a ship named "*Dongfanghong II*", which was designed for multiple disciplines research in marine environment with a ship-based atmospheric science lab. Meteorological data, including time, latitude, longitude, cruising speed and direction, wind speed, wind direction, relative humidity, air pressure and temperature were observed by the meteorological sensors (RM Young, USA) with resolution of 10 seconds, and were used to filter and flag the observed CO_2 and CH_4 mixing ratios and verify simulated wind fields.

2.4 Air mass transport model

HYSPLIT (Hybrid Single Particle Lagrangian Integrated Trajectory Model, HYSPLIT) is developed by the National Oceanic and Atmospheric Administration's Air Resources Laboratory (NOAA-ARL) and the Bureau of Meteorology of Australia, which can simulate the air mass transportation combined with the National Centers for Environmental Prediction (NCEP) reanalysis data. The principle of simulating the air mass transportation path is as follows: assuming that particles in the air are floating in the wind, their moving trajectory is the integral of their position vectors in time and space (Zhang et al., 2011; Xia et al., 2018). Backward trajectory analysis uses the mixed single-particle Lagrangian integral transport and diffusion model to calculate the air particles forward, analyzes the influence of air mass transportation on the spatial and temporal distribution of atmospheric components in the observation area by tracking the transport path, and infer their potential sources. The main parameters required to calculate the backward trajectory are the altitude, latitude and longitude of the starting point. Generally, the calculation is carried for 72 h (Zhan et al., 2009；Zhang et al., 2017; Zhang et al., 2019).

3 Results

3.1 Atmospheric CO_2 and CH_4 mixing ratios

Generally, CO_2 and CH_4 mixing ratios decreasing with increasing altitude and distance away from continent, and decreasing latitude (Matsueda et al., 1996; Bartlett et al., 2003; Zang et al., 2017). Spatiotemporal distributions of atmospheric CO_2 and CH_4 mixing ratios in shelf seas suggested not only natural characteristics, but also multiple anthropogenic processes, such as marine oil and gas exploration (Nara et al., 2014; Zang et al., 2020), land-sea air mass transportation (Kong et al., 2010; Liu et al., 2018), and malfunction of observation instrument (Zang et al., 2017).

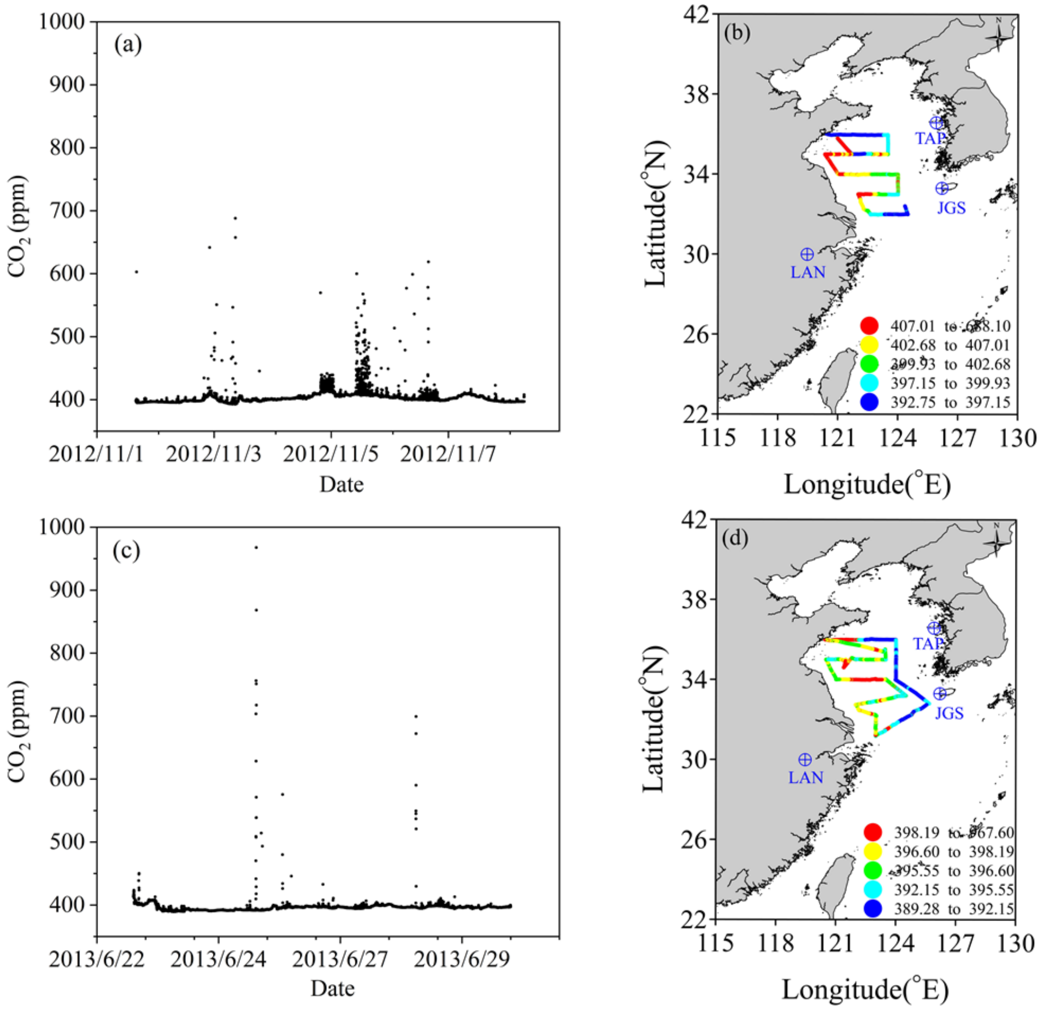

Fig. 3. Temporal（a and c）and spatial （b and d）distribution of CO_2 mixing ratios in November 2012 and June 2013 in the SYS.

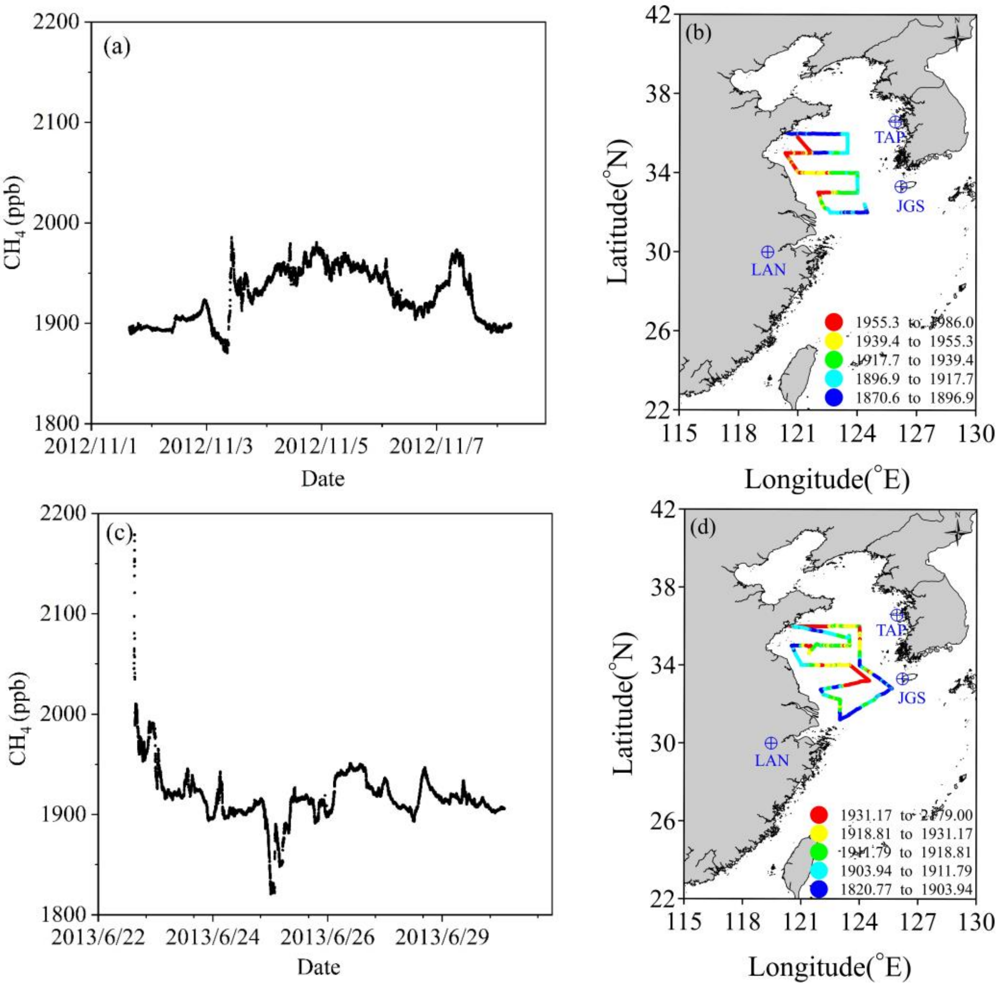

Fig. 4. Temporal (a and c) and spatial (b and d) distribution of CH_4 mixing ratios in November and June of the SYS.

During the two field surveys, atmospheric CO_2 mixing ratios ranged from 392.75 ppm to 688.10 ppm in November 2012 (Fig. 3a and Fig. 3b), and ranged from 389.28 ppm to 967.60 ppm in June 2013 (Fig. 3c and Fig. 3d), respectively. Atmospheric CH_4 mixing ratios ranged from 1870.6 ppb to 1986.0 ppb in November 2012 (Fig. 4a and Fig. 4b), and ranged from 1820.8 ppb to 2179.0 ppb in June 2013 (Fig. 4c and Fig. 4d), respectively. Atmospheric CO_2 and CH_4 mixing ratios were comparable with the historical observation results of the north hemisphere (Matsueda et al., 1996; Zang et al., 2017；Liu et al., 2018). Abnormal high observation values were attributed to exhaust gases of ship or anthropogenic interference of analyzer.

3.2 Wind data

Observed wind data were averaged to hourly data for subsequently analysis. As shown in Fig. 5a, during the survey of November 2012, hourly mean wind speed ranged from 0.05 to 20.46 m/s with an average value of 8.09 (4.17) m/s. Dominate wind direction was from north and northeast, indicated the air masses flowed from the Asia continent to the Pacific Ocean. As shown in Fig. 5c, during the survey of June 2013, hourly mean wind speed ranged from 0.08 m/s to 9.42 m/s with an average value of 4.72 (1.79) m/s. Conversely, the predominant wind direction turned into south or southeast, which promoted air masses flowing from the Pacific Ocean to the Asia continent. In addition, the observed dominant wind directions (Fig. 5a and Fig. 5c) were consisting well with the simulated wind fields (Fig. 5b and Fig. 5d), suggested the typical features of winter and summer monsoon, which were ideal cases to study effects of land-sea air masses transportation on the spatiotemporal variations of CO_2 and CH_4 mixing ratios in the MBL of the SYS.

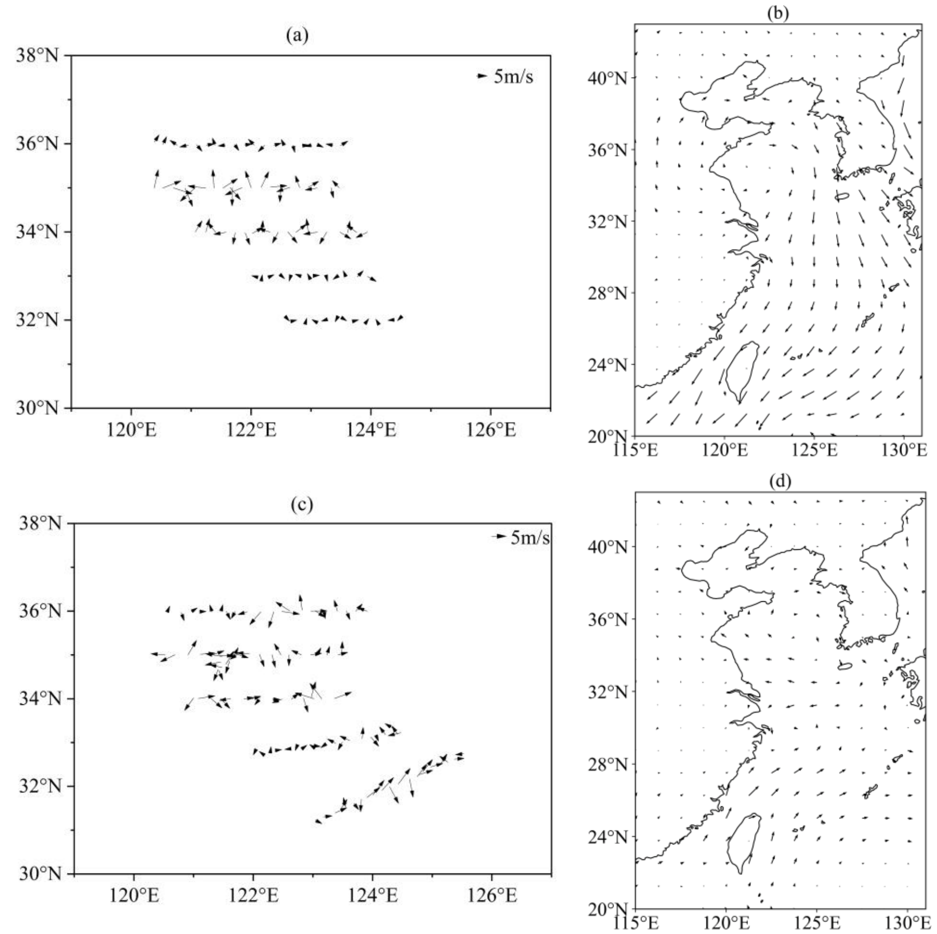

Fig. 5. Observed wind direction and speed (a and c) and simulation of wind fields (b and d) over the SYS. The simulated wind fields were plotted based on the ERA5 hourly data on pressure levels provided by the European Centre for Medium-Range Weather Forecasts (ECMWF), (https://cds.climate.copernicus.eu/cdsapp#!/dataset/reanalysis-era5-pressure-levels?tab=form, download date: 2022-11-04).

4. Discussion

4.1 Data filter approach

Although some empirically based data processes have been reported (Zang et al., 2017; Liu et al., 2018), a specific data filtering approach for shipborne continuous observation need to be optimized and established to distinguish impacts of multiple source-sink processes on shipborne observed atmospheric CO_2 and CH_4 mixing ratios along the cruise tracks, especially in the shelf seas.

Firstly, observed atmospheric CO_2 and CH_4 mixing ratios along the cruise tracks in November 2012 and June 2013 were calibrated by a linear function, averaged every one minute, and named as Raw Data for the subsequently process.

Secondly, according to voyage record, the abnormal values that caused by mal-function of instrument and impacted by manually refilling the drying-tube were flagged (Zang et al., 2017).

Thirdly, when the ship stopping for oceanography investigating at discrete stations or cruising downwind with speed lower than wind speed, observed atmospheric CO_2 and CH_4 mixing ratios might be impacted by ship's exhaust gas and human activities (Zang et al., 2017; Liu et al., 2018). Previous studies considered 3 knots as the criterion to flag data influenced by ship's exhaust gas and human activities by observation experience (Zang et al., 2017; Liu et al., 2018).

In this study, take two station measurement as examples, as showed in Fig. 6a and Fig. 6b, when ship speed slowed down from normal cruising speed of 11 knots to less than 3 knots, the observed CO_2 mixing ratio varied from a smooth pattern with SD (standard deviation) value less than 0.10 ppm to intensive fluctuation pattern with SD value greater than 1.20 ppm, due to influences of ship emissions and human activities. According to the quality control criteria of CO_2 (± 0.10 ppm), which recommended by the World Meteorological Organization Global Atmospheric Watch (WMO/GAW) (WMO 2005), 3 knots was optimized as the threshold. Results showed that, 15.5% and 21.9% of total observed data in November 2012 and June 2013, respectively, were flagged in this step.

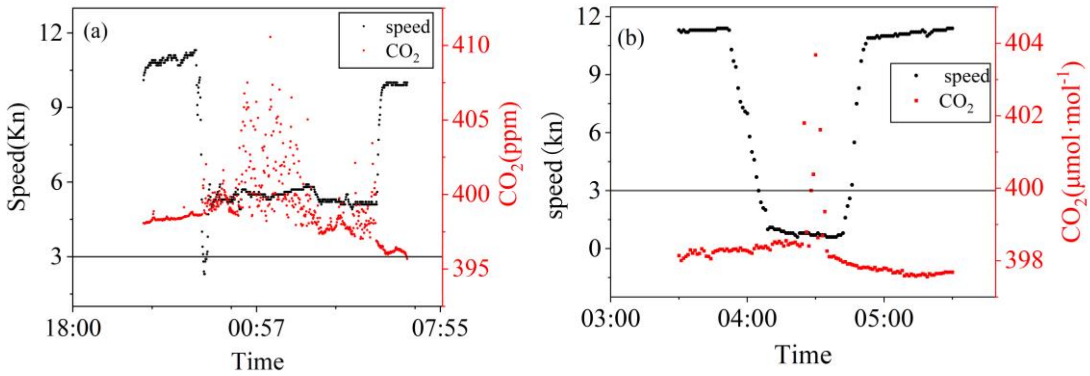

Fig. 6. Variations of observed CO_2 mixing ratios and ship speed from 20:40 on 28th to 6:40 on 29th June 2013 (a) and 3:30 to 5:30 on 3th November 2012(b).

Finally, the Pauta criterion ("3σ" method), a widely used data quality control approach in atmospheric greenhouse gas observation (Zhang et al., 2007; Zhang et al., 2013; Fang et al., 2015; Zang et al., 2017), was introduced to filter and flag the non-background measurement results. To optimize this process, observation data that covered period of 0.5, 1, 2 and 4 hour was calculated, respectively. Any deviation between observed results and average value lying outside ± 3 SD was considered as non-background data and should be flagged. This procedure was repeated until no outliners were identified (Zhang et al., 2007). Result showed that data calculated hourly was optimal, because it could not only flag dispersed values, but keep the smooth data well.

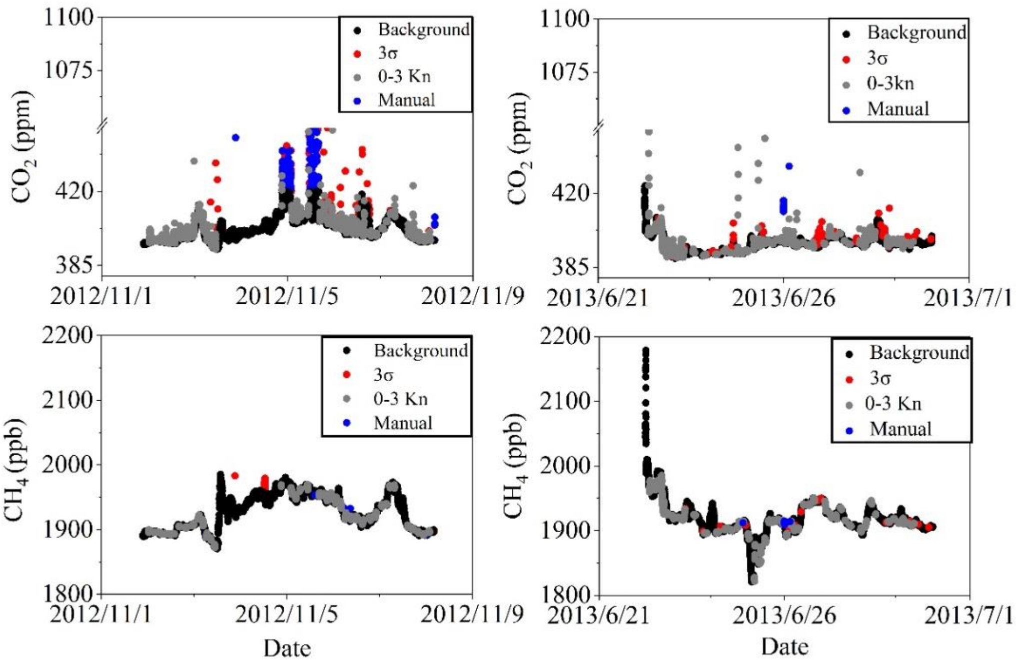

Fig. 7. Filtered results of CO_2 (a, b) and CH_4 (c, d) mixing ratios in November 2012 and June

2013, the ordinates of a and b are broken in the range of 450 to 1050 ppm. Black points represent the background data (Background). Blue points represent data influenced by replacing dry tube that were manually flagged (Manual). Gray points mean the data influenced by ship emissions at low speed (less than 3 knots). Red points represent the data filtered out by the Pauta criterion (3σ).

As shown in Fig. 7, based on the optimized approach, observed data could be filtered and flagged. The remained data accounted for 79.5% and 75.7% of raw data in November 2012 and June 2013, respectively, which were considered as background represents, and used for further analysis.

Observed mean CO_2 mixing ratios were 403.94 (13.77) ppm and 395.90 (3.53) ppm in November 2012 and June 2013, respectively, which were slightly lower than previous studies' mean values of 405 ppm and 410 ppm in the YS and ECS in March 2013 and March 2017, respectively (Zang et al., 2017; Liu et al., 2018). Moreover, observed mean atmospheric CO_2 mixing ratio was almost equal to results observed at the TAP (401.37 ppm) and JGS (403.77 ppm) stations, but approximate 9 ppm higher than MBL-CO_2 reference (394.41 to 394.78 ppm in latitude zone of 30 °N to 37 °N) (https://gml.noaa.gov/ccgg/mbl/data.php download data: 2022-10-10) in November 2012, and almost equal to results observed at the LAN (396.43 ppm) and JGS (398.10 ppm) stations and MBL-CO_2 reference (397.38 to 397.92 ppm in latitude zone of 30 °N to 37 °N) in June 2013.

Observed mean CH_4 mixing ratios were 1924.8 (27.8) ppb and 1918.0 (25.7) ppb in November 2012 and June 2013, respectively, which were slightly higher than historical data of 1915.5 ppb in the SYS in March 2013 (Zang et al., 2017), and higher than the MBL-CH_4 references of November 2012 (1869.5 to 1880.3 ppb) and June 2013 (1835.3 to 1846.6 ppb).

4.2 Influence of air-sea exchange on distribution of atmospheric CO_2 and CH_4 mixing ratios

Air-sea exchange is a dynamic process when CO_2 and CH_4 molecules diffusing via the interface of surface seawater and overlying atmosphere. Source and sink of atmospheric CO_2 and CH_4 mean they were emitted from or absorbed by seawater. In fact, the magnitude of air-sea CO_2 and CH_4 exchange varied dramatically in spatial and temporal scale in coastal shallow seas (Yang et al., 2016; Gao et al., 2019). Generally, CO_2 and CH_4 emitted from the seawater into the air were difficult to trace by atmospheric measurements because they could dilute sharply (Schmale et al., 2005; Kourtidis et al., 2006; Zhai et al., 2013), only shallow seeps areas and coastal regions, could influence mixing ratios of local atmospheric CO_2 and CH_4 directly and be measured (Leifer et al., 2006; Luo et al., 2015). Despite the dissolved CO_2 and CH_4 were not observed in our field surveys, the published data showed that sea-to-air CO_2 fluxes were 6.0 (8.8 mmol/m^2/day in November 2012 and 2.6 (4.3) mmol/m^2/day in June 2011 (Wang and Zhai, 2021), and sea-to-air CH_4 fluxes were 6.4 μmol/m^2/day in November 2002 and 15.7 μmol/m^2/day in June 2006 (Zhang et al., 2008), respectively, in the SYS.

To estimate the effects of air-sea exchange on mixing ratios of atmospheric CO_2 and CH_4, we used a simple method described by Kourtidis et al. (2006) and optimized by Zang et al. (2020): assumed that a box located above the survey area, with a ceiling of 10 meters which corresponding to the height of air inlet in our field surveys. The contents of atmospheric CO_2 and CH_4 were only impacted by air-sea exchange. When CO_2 and CH_4 were vented into or absorbed from the box, their mixing ratios would increase or decrease homogeneously, caused by the mean calculated results of sea-to-air CO_2 and CH_4 fluxes.

Generally, coastal shallow seas are source of atmospheric CH_4, accounting for approximate 75% of global ocean emissions (Bange et al., 1994; Bates et al., 1996). However, according to the calculation formula that given by Zang et al. (2020), sea-to-air CH_4 flux of 50.8 μmol/m^2/day could result in an increasing of 2 ppb of atmospheric CH_4 mixing ratio in the MBL. Thus, the impacts of the reported mean sea-to-air CH_4 fluxes (6.4 μmol/m^2/day and 15.7 μmol/m^2/day in November 2002 and June 2006) on the atmospheric CH_4 would not exceed 1 ppb (Zhang et al., 2008). In addition, based on the same method, the impacts of the reported mean sea-to-air CO_2 fluxes (Wang and Zhai, 2021) on the atmospheric CO_2 mixing ratios were calculated, which was no more than 14.1 ppb. Thus, it was reasonable to conclude that influences of air-sea exchange on distribution of atmospheric CO_2 and CH_4 mixing ratios were slight or negligible, compared to the observed variability of atmospheric CO_2 and CH_4 (Fig.3 and Fig. 4).

4.3 Influences of land–sea air mass transportation on spatiotemporal distribution of atmospheric CO_2 and CH_4 mixing ratios

The EAWM is closely related to atmospheric compounds transportation from the Asia Continent to the Western Pacific (Yu et al., 2014). Since two surveys were conducted in November 2012 and June 2013, when the typical winter and summer monsoon season in their early phases, respectively (Lyu et al., 2021; Lin'an et al., 2022), the observation data could give us an ideal opportunity to study the impacts of land-to-sea air mass transportation on spatiotemporal distribution of atmospheric CO_2 and CH_4 mixing ratios over the SYS. Observed atmospheric CO_2 and CH_4 mixing ratios were higher in November 2012 (Fig. 8) than that in July 2013 (Fig. 9). Except for the Section 1 (S1) and the right end of Section 2 (S2), the spatial distributions were gradient descent with offshore distance (Fig. 8).

In situ observed data demonstrated that the dominant wind direction was W-NW-NNW for section 2, 3, 4 and 5 in November 2012, suggested the air masses were transported from the Asian Continent to the Pacific Ocean (Fig. 5 and Supplementary data). Generally, CO_2 and CH_4 mixing ratios were higher in continent than that of the MBL (Zhang et al., 2007; Zang et al., 2017; Liu et al., 2018), land-to-sea air mass transportation driven by the EAWM could result in the horizontal transmission of greenhouse gases. Due to the subsequently mixing and dilution, CO_2 and CH_4 mixing ratios would decline along the windward (Bartlett et al., 2003; Kourtidis et al., 2006; Liu et al., 2018). Meanwhile, the mixing ratios of atmosphere CO_2 and CH_4 were low and homogeneous in Section 1 and right end of Section 2, because the dominant wind direction was ENE-SE-S, indicated air masses were transported from the open Pacific Ocean with low content of CO_2 and CH_4 (Matsuda, 1996; Bartlett et al., 2003; Zang et al., 2017).

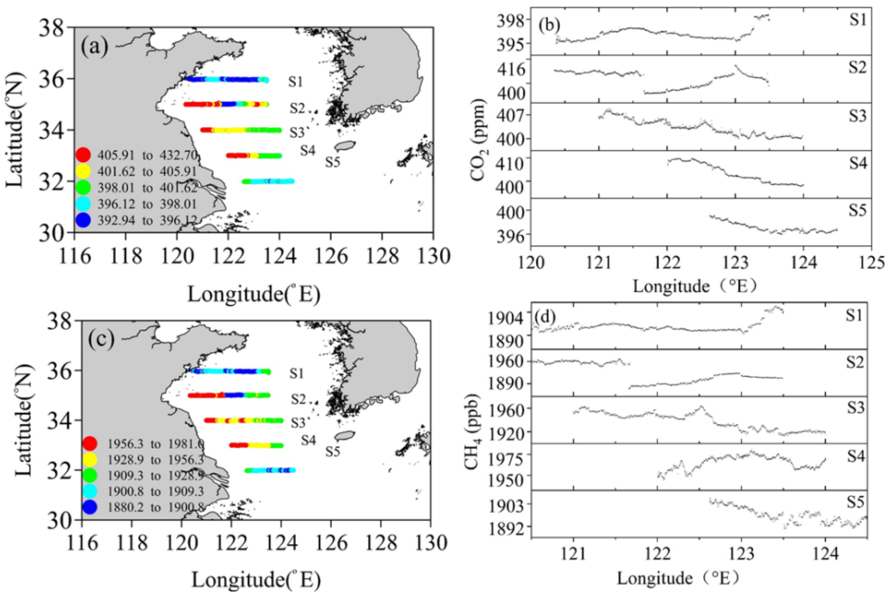

Fig. 8. Spatial distributions of CO_2 and CH_4 mixing ratios in the survey area in November 2012.

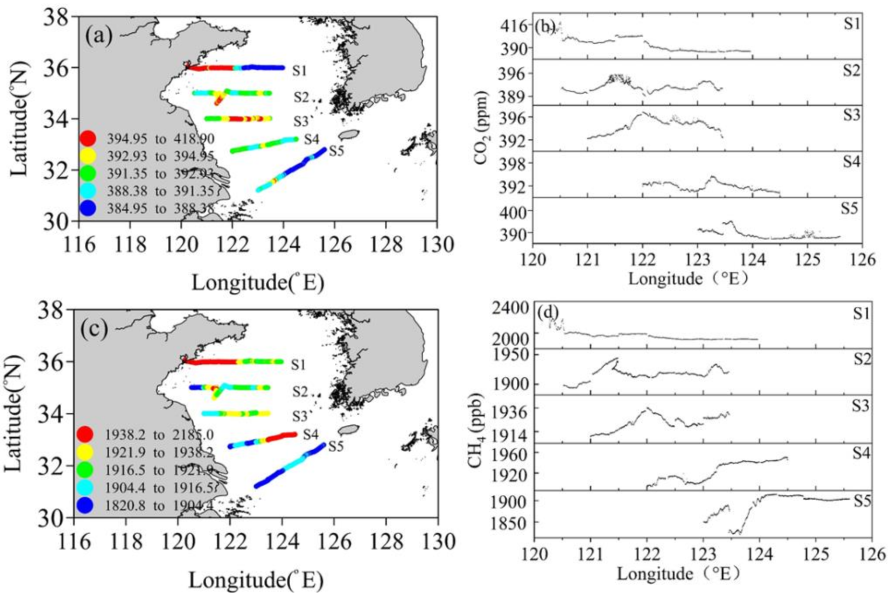

Fig. 9. Spatial distributions of CO_2 and CH_4 mixing ratios in the survey area in July 2013.

Furthermore, back trajectory analysis showed that almost all the transport tracks were originated from the Asian Continent in November 2012, and the South China Sea and West Pacific Ocean in July 2013 (typical characteristics of the early summer monsoon) (Fig. 10), which resulted in higher atmospheric CO_2 and CH_4 mixing ratios in November 2012 (Fig. 8) than that in July 2013 (Fig. 9). Seasonal variations of atmospheric CO_2 and CH_4 mixing ratios were consistent with the variations of atmospheric CO_2 mixing ratios in West Pacific Ocean, where atmospheric components distributions were dominated by maritime air masses from the Pacific Ocean and polluted air masses from the Asian Continent (Matsuda, 1996; Zhang et al., 2007; Liu et al., 2018).

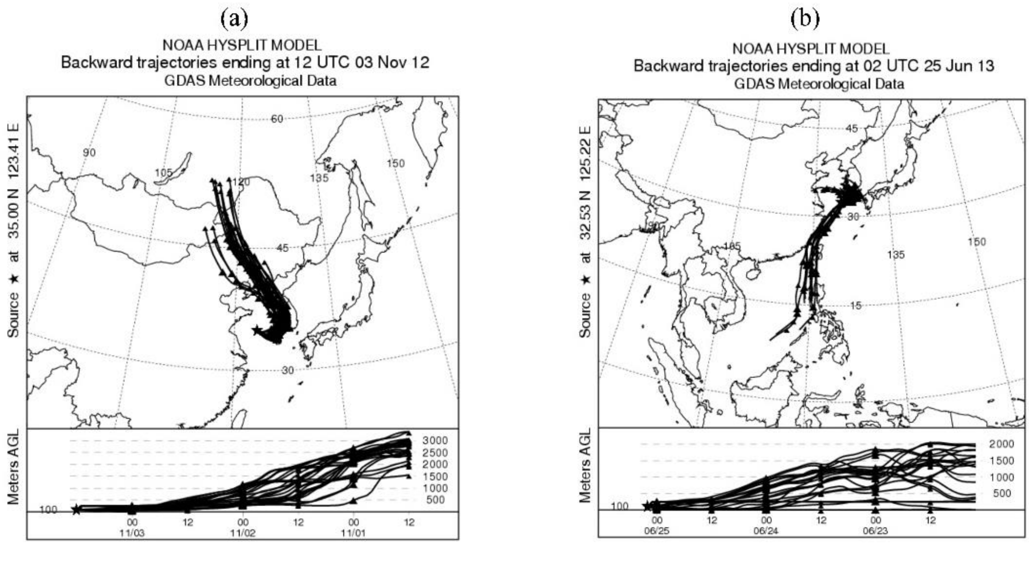

Fig. 10. Three-day air back-trajectories of two typical locations, a (35.00 °N, 123.41 °E) and b

(32.53 °N, 125.22 °E).

4.4 Estimated distance of land-to-sea air mass transportation

As shown in Fig. 11, atmospheric CO_2 and CH_4 mixing ratios observed in November 2012 showed the same fluctuating feature versus wind direction, indicated their variations were dominated by the land-to-sea air masses transportation, which was in agreement with previous studies (Zhang et al., 2007; Zang et al., 2017; 2020; Liu et al., 2018).

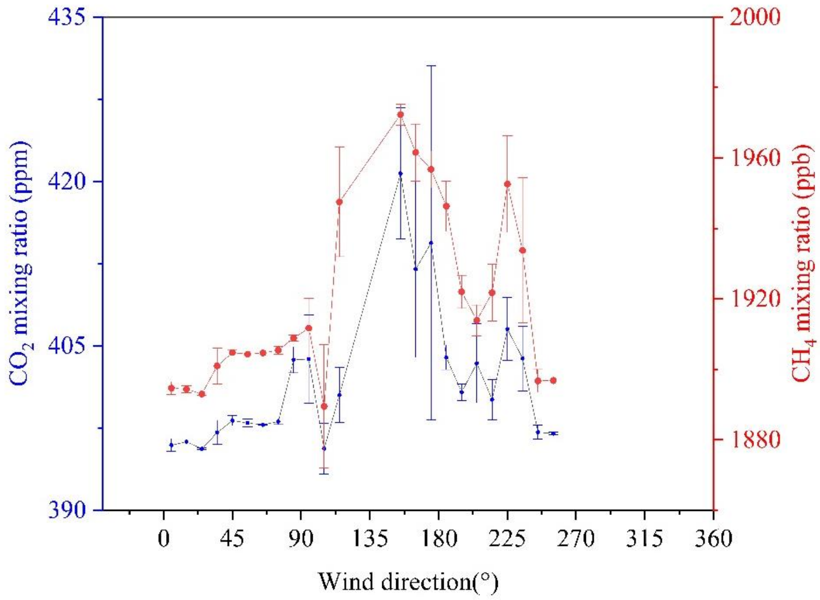

Fig. 11. Relationship between wind direction and atmospheric mixing ratios of CO_2 and CH_4, respectively. Error bars indicated standard deviations in each wind direction.

Simulation studies of gas seeps in the Black Sea and the Nord Stream pipeline gas leaks in the Baltic Sea showed that atmospheric CH_4 mixing ratio could be enhanced by the upwind emission source in distance of 5 to 30 km (Kourtidis et al., 2006; Jia et al., 2022). NOAA's MBL-CO_2 and MBL-CH_4 references were 394.56 ppm and 1875.4 ppb, respectively, at the same latitude zone with the survey area in November 2012. ΔCO_2 and ΔCH_4 represented deviations between observed atmospheric CO_2 and CH_4 mixing ratios and MBL-CO_2 and MBL-CH_4 references. As shown in Fig. 12, we assumed that the effects of mixing and dilution during the transportation was linear (Kourtidis et al., 2006), the further the observation site away from continent, the lower the ΔCO_2 and ΔCH_4 values in each survey section. According to the calculated slope values, gradient would be gradual at 123.30 °E, 123.50 °E and 123.40 °E for section 3, 4 and 5, respectively. Moreover, the offshore distances away from continent could be calculated as approximate 27.0, 26.3 and 11.7 km, respectively, with a mean value of 21.7 km. Thus, spatial distributions of atmospheric CO_2 and CH_4 mixing ratios in the China shelf sea could be impacted remarkably by land-to-sea air mass transportation during early phase of the EAWM.

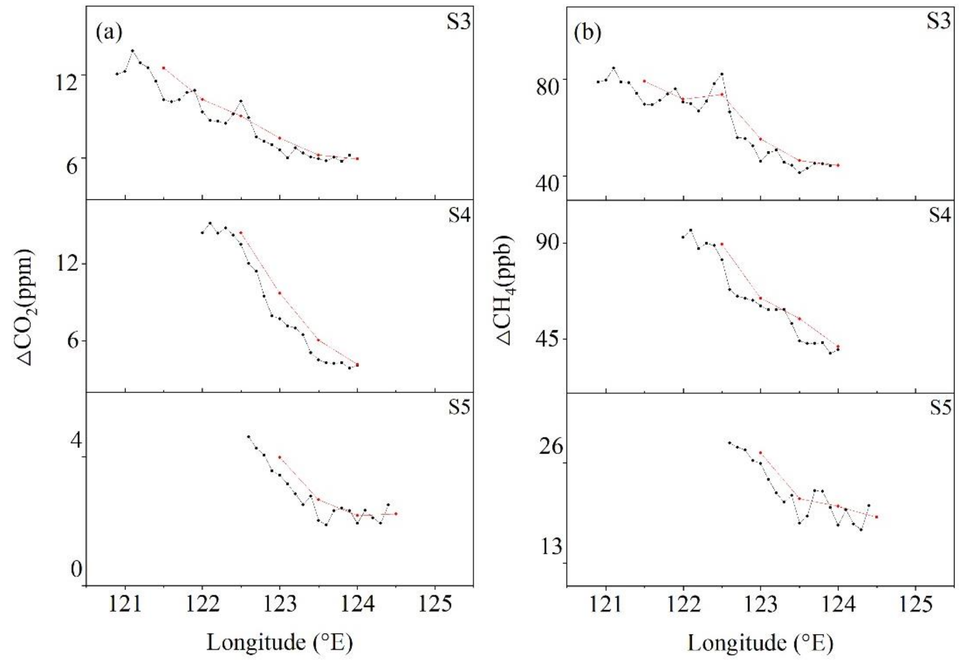

Fig. 12. The average value of ΔCO_2 (a) and ΔCH_4 (b) per 0.1 (black) or 0.5 longitude (red) in November 2012.

5. Conclusions

Based on the shipborne continuously observed atmospheric CO_2 and CH_4 mixing ratios and meteorological parameters over the SYS in November 2012 and June 2013, a data filter method was optimized and established, which could be used to flag CO_2 and CH_4 mixing ratios influenced by multiple natural processes and human activities. Spatial and seasonal variations of atmospheric CO_2 and CH_4 mixing ratios over the SYS were mainly regulated by the EAM, while the influence of air-sea exchange was slight or negligible. Summer monsoon resulted in relatively low atmospheric CO_2 and CH_4 mixing ratios with a gradient increasing from southeast to northwest. Conversely, winter monsoon enhanced land-to-sea air masses transportation with high atmospheric CO_2 and CH_4 mixing ratios, which induced decreasing patterns with increasing distance offshore. Effect of land-to-sea air mass transportation on enhanced CO_2 and CH_4 mixing ratios was quantification with a distance of approximate 20 km offshore during the early period of the EAWM.

Code availability. The code that is used for figure plotting (python) can be provided upon request.

Data availability. The ERA5 hourly data on pressure levels provided by the European Centre for Medium-Range Weather Forecasts (ECMWF), https://cds.climate.copernicus.eu/cdsapp#!/dataset/reanalysis-era5-pressure-levels?tab=form, download date: 2022-11-04). The simulated MBL values produced by NOAA, www.esrl.noaa.gov/gmd/ccgg/GHGreference, download data: 2022-10-10.

Author contributions

Jiaxin Li prepared the main part of the paper and performed the corresponding analyses. Kunpeng Zang provided the original data that are used within this study and helped with the data analyses and the preparation of the paper. Yi Lin, Yuanyuan Chen, Shuo Liu, Honghui Xu and Yujun Jiang provided valuable comments on data processing and, as well as help in the drawing of Fig. 5. Shuangxi Fang, Shanshan Qiu and kai Jiang suggestions for revising the paper and further standardized the paper. Haoyu Xiong, Xuemei Qing and Haixiang Hong helped download the MBL-references data.

Competing interest

This manuscript is approved by all authors for publication, and we have no competing interests to declare that are relevant to the content of this article.

Acknowledgments

The authors wish to thank the crew of the R/V "Dongfanghong II" for their assistance on board. We also thank Dr. E. J. Dlugokencky and colleagues from the Tae-ahn Peninsula station， Jeju Gosan station and Lin'an station. This work was supported by the National Key Research and Development Program of China (2020YFA0607501), the National Natural Science Foundation of China (No. 42275113), the Special Support Plan for High-level Talents in Zhejiang province (2021R542048), the Joint funds of the Zhejiang Provincial Natural Science Foundation of China under Grant No. LZJMZ23D050002, the Fund of Key Laboratory of Global Change and Marine-Atmospheric Chemistry, MNR (GCMAC2001) and the Basic Public Welfare Research Program of

Zhejiang Province (LGF22D050004).

References

AGGI. The NOAA annual greenhouse gas index (AGGI). NOAA Earth System Research Laboratory, Boulder, Colorado, USA. http://esrl.noaa.gov/gmd/aggi/aggi.html, 2014.

Bange, H. W., Bartell, U. H., Rapsomanikis, S., and Andre, M. O.: Methane in the Baltic and North Seas and a Reassessment of the Marine Emissions of Methane, Global Biogeochem Cy., 8, 465-480, https://doi.org/10.1016/j.marchem.2008.02.005, 1994.

Bartlett, K. B., Sachse, G. W., Slate, T., Harward, C., and Blake, D. R.: Large-scale distribution of CH_4 in the western North Pacific: Sources and transport from the Asian continent, J. Geophys. Res-Atmos., 108, D20, https://doi:10.1029/2002JD003076, 2003.

Bouman, E. A., Lindstad, E., Rialland, A. I., and Stomman, A. H.: State-of-the-art technologies, measures, and potential for reducing GHG emissions from shipping-A review, Transport. Res. D-Tr. E, 52, 408-421, http://dx.doi.org/10.1016/j.trd.2017.03.022, 2017.

Chang, C., L. Yi, and Chen, G. T.: A numerical simulation of vortex development during the 1992 east Asian summer monsoon onset using the navy's regional model, Mon. Wea. Rev., 128, 1604–1631, https://doi.org/10.1175/1520-0493(2000)128<1604:ANSOVD>2.0.CO;2, 2000.

Crosson, E. R.: A cavity ring-down analyzer for measuring atmospheric levels of methane, carbon dioxide, and water vapor, App. Phys. B-Lasers. O., 92, 403-408, https://10.1007/s00340-008-3135-y, 2008.

Dlugokencky, E. J., Myers, R. C., Lang, P. M., Masarie, K. A., Crotwell, A. M., Thoning, K. W., Hall, B. D., Elkins, J. W., and Steele, L. P.: Conversion of NOAA atmospheric dry air CH_4 mole fractions to a gravimetrically prepared standard scale, J. Geophys. Res., 110, D18306, https://doi.org/10.1029/2005JD006035, 2005.

Ding, Y. H., Liu, J. J., Sun, Y., Liu, Y., He, J., and Song, Y.: A study of the synoptic-climatology of the Meiyu system in East Asia, Chinese Journal of Atmospheric Sciences, 31, 1082-1101, 2007.

Ding, J., Van Der A, R. J., Mijling, B., Jalkanen, J. P., Johansson, L., and Levelt, P. F.: Maritime NOx emissions over Chinese Seas derived from satellite observations, Geophys. Res. Lett., 45, 2031-2037, https://doi.org/10.1002/2017GL076788, 2018.

Fang, S. X., Zhou, L. X., Masarie, K. A., Xu, L., and Rella, C. W.: Study of atmospheric CH_4 mole fractions at three WMO/GAW stations in China, J. Geophys. Res-Atmos., 118, 4874-4886, https://doi.org/10.1002/jgrd.50284, 2013.

Fang, S. X., Tans, P. P., Steinbacher, M., Zhou, L. X., and Luan, T.: Comparison of the regional CO_2 mole fraction filtering approaches at a WMO/GAW regional station in China, Atmos. Meas. Tech., 8, 5301-5313, https://doi.org/10.5194/amt-8-5301-2015, 2015.

Gao, Z. M., Liu, H. P., and Mcfarland, D. P.: Mechanistic links between underestimated CO_2 fluxes and non-closure of the surface energy balance in a semi-arid sagebrush ecosystem, Enviro. Res. Lett., 14, 1748-9326, https://doi.org/10.1088/1748-9326/ab82d, 2019.

Huang, R. H.: The influence of the heat source anomaly over Tibetan Plateau on the northern hemispheric circulation anomalies, Acta. Meteorol. Sin., 43, 208-220, 1985.

Houghton, R. H., Zhou, L. T., and Chen, W.: The progresses of recent studies on the variabilities of the East Asian monsoon and their causes, Adv. Atmos. Sci., 20, 55-69, 2003.

Jia, M., Li, F., Zhang, Y. Z., Wu, M. S., Li, Y. S., Feng, S. Z., Wang, H. M., Chen, H. L., Ju, W. M., Lin, J., Cai, J. W., Zhang, Y. G., and Jiang, F.: The Nord Stream pipeline gas leaks released approximately 220,000 tonnes of methane into the atmosphere, Environmental Science and Ecotechnology, 12, 2666-4984, https:// doi.org/10.1016/j.ese.2022.100210, 2022.

Kourtidis, K., Kioutsioukis, I., McGinnis, D. F., and Rapsomanikis, S.: Effects of methane outgassing on the Black Sea atmosphere, Atmos. Chem. Phys., 6, 5173–5182, https://doi.org/10.5194/acp-6-5173-2006, 2006.

Kong, S., Lu, B., Han, B., Bai, Z. P., Xu, Z., You, Y., Jin, L. M., Guo, X. Y., and Wang, R.: Seasonal variation analysis of atmospheric CH_4, N_2O and CO_2 in Tianjin offshore area. Sci. China Earth Sci., 53, 1205–1215, https:// doi: 10.1007/s11430-010-3065-5, 2010.

Law, C. S., Brévière, E., De Leeuw, G., Garçon, V., Guieu, C., Kieber, D. J., Kontradowitz, S., Paulmier, A., Quinn, P. K., Saltzman, E. S., Stefels, J., and Von Glasow, R.: Evolving research directions in Surface Ocean-Lower Atmosphere (SOLAS) science, Environ. Chem., 10, 1-16, https://doi.org/10.1071/EN12159, 2013.

Luo, X. F., Wei, H., Liu, Z., and Zhao, L.: Seasonal variability of air–sea CO_2 fluxes in the Yellow and East China Seas: A case study of continental shelf sea carbon cycle model, Cont. Shelf. Res., 107, 69-78, http://dx.doi.org/10.1016/j.csr.2015.07.009, 2015.

Liu, Y. S.，Zhou, L. X., Tans, P. P., Zang, K. P., and Cheng, S. Y.: Ratios of greenhouse gas emissions observed over the Yellow Sea and the East China Sea, Sci. Total. Environ., 33, 1022-1031 https://doi.org/10.1016/j.scitotenv.2018.03.250, 2018.

Lyu, W. Z., Fu, T. F., Hu, Z. X., Tang, Y. Z., Chen, G. Q., Xu, X. Y., Chen, Y. P., and Chen, S. L.: Sedimentary dynamics of the central South Yellow Sea revealing the relation between east Asian Summer and Winter Monsoon over the past 6000 years, Front. Earth Sci., 9, 689508, https://doi.org/10.3389/feart.2021.689508, 2021.

Masarie, K. A., and Tans, P. P.: Extension and integration of atmospheric carbon-dioxide data into a globally consistent measurement record. J. Geophysl. Res-Atmos., 100, 11593-11610, https://doi.org/10.1029/95JD00859, 1995.

Matsueda, H., Inoue, H. Y., Ishii, M., and Nogi, Y.: Atmospheric methane over the North Pacific from 1987 to 1993. Geochem. J., 30, 1-15, 1996.

Nara, H., Tanimoto, H., Tohjima, Y., Mukai, H., Nojiri, Y., and Machida, T.: Emissions of methane from offshore oil and gas platforms in Southeast Asia, Sci Rep 4, 6503, https://doi.org/10.1038/srep06503, 2014.

Peters, G., Marland, G., Le Quéré, C., Boden, T., Canadell, J. G., and Raupach, M. R.: Rapid growth in CO_2 emissions after the 2008-2009 global financial crisis, Nat. Clim. Change., 2, 2–4, https://doi.org/10.1038/nclimate1332, 2012.

Rella, C. W., Chen, H., Andrews, A. E., Filges, A., Gerbig, C., Hatakka, J., Karion, A., Miles, N. L., Richardson, S. J., Steinbacher, M., Sweeney, C., Wastine, B., and Zellweger, C.: High accuracy measurements of dry mole fractions of carbon dioxide and methane in humid air, Atmos. Meas. Tech., 6, 837–860, https://doi.org/10.5194/amt-6-837-2013, 2013.

Riddick, S. N., Mauzerall, D. L., Cella, M., Harris, N. R. P., Allen, G., Pitt, J., Staunton-Sykes, J., Forster, G. L., Kang, M., Lowry, D., Nisbet, E. G., and Manning, A. J.: Methane emission from oil and gas platforms in the North Sea. Atmos. Chem. Phys., 19, 9787-9796, https://doi.org/10.5194/acp-19-9787-2019, 2019.

Schmale, O., Greinert, J., and Rehder, G.: Methane emission from high-intensity marine gas seeps in the Black Sea into the atmosphere, Geophys. Res. Lett., 32, 7, https://doi.org/10.1029/2004GL021138. 2005.

Warneke, T., De Beek, R., Buchwitz, M., Notholt, J., Schulz, A., Velazco, V., and Schrems, O.: Shipborne solar absorption measurements of CO_2, CH_4, N_2O and CO and comparison with SCIAMACHY WFM-DOAS retrievals, Atmos. Chem. Phys., 5, 2029–2034, https://doi.org/10.5194/acp-5-2029-2005, 2005.

WMO, 12^{th} WMO/IAEA Meeting of experts on carbon dioxide concentration and related tracers measurement techniques. NO. 161[R]. Toronto, Canada, 2005.

Wang, S. Y., and Zhai, W. D.: Regional differences in seasonal variation of air-sea CO_2 exchange in the Yellow Sea. Cont. Shelf. Res., 218, 104393, https://doi.org/10.1016/j.csr.2021.104393, 2021.

WMO. Greenhouse Gas Bulletin: The state of greenhouse gases in the atmosphere based on global observations through 2021. http:// www.wmo.int/pages/prog/arep/gaw/ghg/ghgbull06en.html , 2022.

Xia, L. J., Liu, L. X., Li, B. Z., and Zhou, L. X.: Spatial and temporal distribution characteristics of atmospheric CO_2 in central China, China Environmental Science, 38, 2811-2819, https://doi.org/10.19674/j.cnki.issn1000-6923.2018.0294, 2018.

Yu, G., Chen, Z., Piao, S. L., Peng, C. H., Ciais, P., Wang, Q. F., Li, X. R., and Zhu, X. J.: High carbon dioxide uptake by subtropical forest ecosystems in the East Asian monsoon region. Proc. Natl. Acade. Sci. U. S., 111, 4910-4915, https://doi.org/10.1073/pnas.1317065111, 2014.

Yang, M., Bell, T. G., Hopkins, F. E., Kitidis, V., Cazenave, P. W., Nightingale, P. D., Yelland, M. J., Pascal, R. W., Prytherch, J., Brooks, I. M., and Smyth, T. J.: Air–sea fluxes of CO_2 and CH_4 from the Penlee Point Atmospheric Observatory on the south-west coast of the UK, Atmos. Chem. Phys., 16, 5745–5761, https://doi.org/10.5194/acp-16-5745-2016, 2016.

Zhan, L. Y.， and Chen, L. Q.: Distribution characteristics of atmospheric nitrous oxide in the Southern Ocean, Chinese Journal of Polar Research, 2007, 49-60, 2007.

Zhan, R. F., and Li, J. P.: Influence of atmospheric heat sources over the Tibetan Plateau and the tropical western North Pacific on the inter-decadal variations of the stratosphere-troposphere exchange of water vapor, Sci. China Ser. D-Earth Sci., 51, 1179-1193, https://doi.org/10.1007/s11430-008-0082-8, 2008.

Zhang, G. L., Zhang, J., Ren, J. L., Li, J. B., and Liu, S. M.: Distributions and sea-to-air fluxes of methane and nitrous oxide in the North East China Sea in summer, Mar. Chem., 110, 42-55, https://doi.org/10.1016/j.marchem.2008.02.005, 2008.

Zhan, M. J., Sun, J. Y., Zhang, Y. M., Zhang, X. C., Nie, H., Deligeer, Kivekas, N., and Lihavainen, H.: The influence of air mass sources on the particle number concentration and the size distribution at Mt.Waliguan, Journal of Glaciology and Geocryology, 31, 659-663, 2009.

Zang, K. P., Zhao, H. D., Wang, J. Y., Xu, X. M., Huo, C., and Zheng, N.: High-resolution measurement of CH_4 in sea surface air based on cavity ring-down spectroscopy technique: the first trial in China Seas. Acta Scientiae Circumstantiate, 33, 1362-1366, 2013.

Zhang, F., Chen, Y. J., Tian, C. G., Wang, X. P., Huang, G. P., Fang, Y., and Zong, Zheng.: Identification and quantification of shipping emissions in Bohai Rim, China, Sci Total Environ, 497-498, 570-577, https://doi.org/10.1016/j.scitotenv.2014.08.016, 2014.

Zhai, W. D.: Sea surface partial pressure of CO_2 and its controls in the northern south China Sea in the non-bloom period in spring, Haiyang Xuebao, 37, 31-40, https:// doi: 10.3969/j.issn.0253-4193.2015.06.004, 2015.

Zhang, J. Y., Song, S. H., Xu, R., and Wen, J. H.: Source of airborne particulate matter in Guilin based on backward trajectory model, Environmental Monitoring in China, 33, 42-46, https://10.19316/j.issn.1002-6002.2017.02.07, 2017.

Zang, K. P., Zhou, L. X., and Wang, J. Y.: Carbon Dioxide and Methane in the China Sea Shelf Boundary

Layer observed by Cavity Ring-Down Spectroscopy, J. Atmos. and Ocean. Tech., 34, 2233-2244, https://doi.org/10.1175/JTECH-D-16-0217.1, 2017.

Zhang, Z. P., and Chu, Z. X.: Modern variations in clay minerals in mud deposits of the Yellow and East China Seas and their geological significance, Holocene, 28, 386-395, https://doi.org/10.1177/0959683617729446, 2018.

Zou, L., Hu, B., Li, J., Dou, Y. G., Xie, L. H., and Dong, L.: Middle Holocene Organic Carbon and biomarker records from the South Yellow Sea: relationship to the East Asian Monsoon, J. Ocean Univ. China, 17, 823-834, https://doi.org/10.1007/s11802-018-3521-y, 2018.

Zhang, Y., Deng, F., Man, H., Fu, M., Lv, Z., Xiao, Q., Jin, X., Liu, S., He, K., and Liu, H.: Compliance and port air quality features with respect to ship fuel switching regulation: a field observation campaign, SEISO-Bohai, Atmos. Chem. Phys., 19, 4899–4916, https://doi.org/10.5194/acp-19-4899-2019, 2019.

Zang, K. P., Zhang, G., Xu, X. M., and Yao, Z. W.: Impact of air-sea exchange on the spatial distribution of atmospheric methane in the Dalian Bay and adjacent coastal area, China, Chemosphere, 251, 126412, https://doi.org/10.1016/j.chemosphere.2020.126412, 2020.